JOURNAL OF SOLID STATE CHEMISTRY 2, 299–302 (1970)

Semiconductor to Metal Transition in $MoTe_2$

M. B. VELLINGA*, R. DE JONGE†, AND C. HAAS

Laboratory for Inorganic Chemistry, State University, Groningen, Netherlands

Received February 16, 1970

$MoTe_2$ undergoes a transition from a diamagnetic, semiconducting phase (α) to a metallic, pauliparamagnetic phase (β). The homogeneity region of the two phases lies between $MoTe_{1.90}$ and $MoTe_{1.99}$. The transition temperature is 820°C for Te-rich samples, and 880°C for Mo-rich samples.

In order to avoid evaporation of Te, electrical resistivity measurements at high temperatures were carried out in a closed vessel, with the sample in equilibrium with its own vapour pressure.

The properties of α- and β-$MoTe_2$ are discussed in terms of a schematic energy level diagram.

Introduction

Several transition-metal compounds show a transition from a semiconducting to a metallic phase (*1–3*). In most cases the transition is accompanied by a change of symmetry of the crystal, in some cases also by a change of composition [CrS (*4*)]. The nature of these transitions is quite different in different compounds, and several theories have been proposed to explain the observed phenomena (*1–3*).

$MoTe_2$ undergoes at about 850°C a transition from the low-temperature diamagnetic, semiconducting α-phase to the high-temperature pauliparamagnetic, metallic β-phase. In α-$MoTe_2$ the metal atoms are surrounded by a trigonal prism of tellurium atoms, in β-$MoTe_2$ the metal atoms have a distorted octahedral coordination. Thus, the structure and physical properties of α-$MoTe_2$ are analogous to those of the disulfides and diselenides of Mo and W, whereas the structure and physical properties of β-$MoTe_2$ are similar to those of WTe_2.

This paper discusses the properties of $MoTe_2$ reported in the literature,[1] and presents some new experimental data. The changes of the physical properties at the transition point are discussed in terms of the energy levels for *d*-electrons of metal atoms with octahedral and trigonal-prismatic coordination.

Experimental Data

A. Phase Diagram

Spiesser and Rouxel report a homogeneity region of $MoTe_2$ between $MoTe_{1.75}$ and $MoTe_2$ (*6*). Our data indicate a narrower homogeneity region.

$MoTe_2$ was prepared by heating weighed amounts of the oxygen free elements for one week at temperatures between 600 and 1000°C. Compositions corresponding to the tellurium- and molybdenum-rich limits of the homogeneity region were prepared by bringing the samples in equilibrium with mixtures of $MoTe_2$ + Te and $MoTe_2$ + Mo_3Te_4, respectively, at temperatures between 750 and 950°C. The composition of the samples was determined by chemical analysis. From these experiments the homogeneity region was found to lie between $MoTe_{1.90}$ and $MoTe_{1.99}$ at temperatures between 750 and 950°C.

The phase transition from the α- to the β-phase was observed on high-temperature X-ray photographs, using a Guinier–Lenné camera. The onset of the transition is at 820°C for the tellurium-rich samples, and at 880°C for the molybdenum-rich samples, according to DTA-measurements. The β-phase can be obtained at room temperature by quenching. On heating, the metastable β-phase transforms at about 500°C to the α-phase.

*† Present address: Central Laboratory DSM, Geleen, Netherlands.

[1] A thorough review of the properties of transition-metal dichalcogenides has been published recently (*5*).

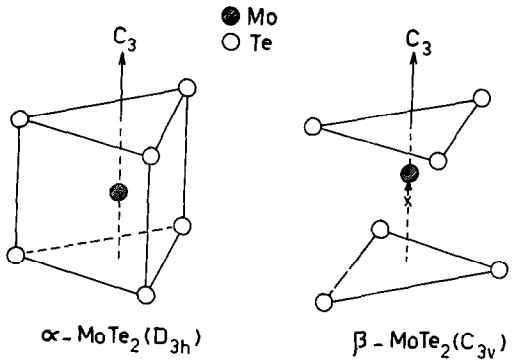

FIG. 1. Coordination of Mo atoms in α- and β-$MoTe_2$.

B. Crystal Structure

α-$MoTe_2$ crystallizes in the MoS_2-structure, a layer-type structure with metal atoms surrounded by a trigonal prismatic arrangement of six chalcogen atoms (*7*) (Fig. 1a). β-$MoTe_2$ has a layer-type structure with the metal atoms in octahedra of chalcogen atoms. The metal atoms are not in the centers of the octahedra, but are shifted in the direction of an octahedron face (Fig. 1b), in such a way that metal–metal zigzag chains are formed (*8*).

C. Electrical Properties

Metallic conductivity with a temperature-independent resistivity of 10^{-3} Ω cm has been reported for β-$MoTe_2$ (*9*). α-$MoTe_2$ is a semiconductor with resistivities at 300°K ranging from 1 Ω cm [single crystal data (*10*)] to 10^3 Ω cm [polycrystalline material (*9*)]. The data reported in the literature are not reproducible at higher temperatures (above 300°C) due to the evaporation of tellurium from the sample.

In order to eliminate changes of composition due to the evaporation of tellurium, we carried out measurements of the resistivity in a specially constructed closed sample holder, containing a polycrystalline bar of $MoTe_2$ in equilibrium with its own vapour pressure. Polycrystalline bars of α-$MoTe_2$ were obtained by pressing with a pressure of 5 tons/cm^2 at room temperature, and subsequent sintering during one week at 780°C. Bars of β-$MoTe_2$ were only pressed, not sintered.

A plot of the resistivity ρ vs $1/T$ for α-$MoTe_2$ (Fig. 2) shows a semiconducting behaviour up to the transition point with an activation energy of 0.6 eV. This activation energy is about half the value of the energy gap, obtained from optical absorption data (*11*). At the transition point there is an abrupt decrease of the resistivity from 2×10^{-2} Ωcm (α) to 10^{-3} Ωcm (β). Measurements of the thermoelectric

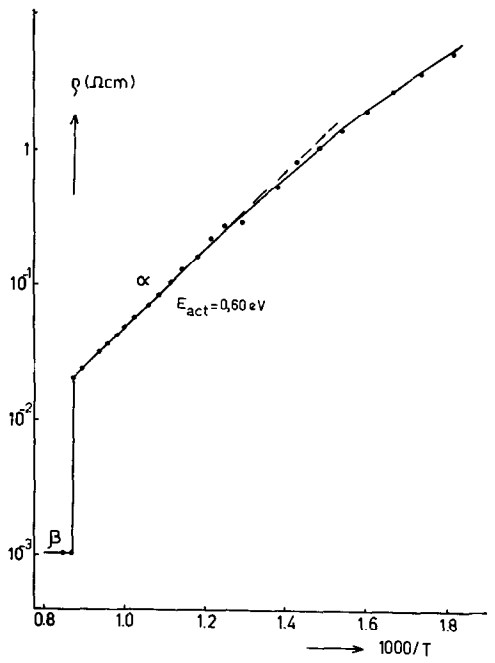

FIG. 2. Resistivity ρ versus reciprocal temperature for α- and β-$MoTe_2$. The phase transition corresponds to an abrupt change of ρ at 1175°K.

power S of α-$MoTe_2$ show some samples to be *n*-type, some *p*-type, with values of S ranging from 100 to 600 μV/°K.

For a quenched sample of β-$MoTe_2$ a resistivity at room temperature of 5×10^{-4} Ω cm was obtained (Fig. 3).[2] The thermoelectric power of β-$MoTe_2$ is positive, with $S = +22\mu$V/°K at 300°K. The electrical properties of β-$MoTe_2$ show no systematic depend-

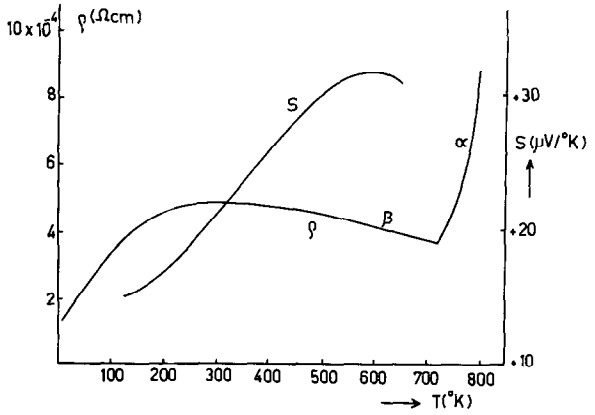

FIG. 3. Resistivity ρ and thermoelectric power S as a function of temperature for metastable β-$MoTe_2$. The rapid increase of ρ at 750°K corresponds to a transformation into the α-phase.

ence on the composition. Essentially, the same results are obtained for tellurium-rich and molybdenum-rich samples. This result shows that β-$MoTe_2$ is a true metal, i.e., the charge carriers do not originate from deviations from stoichiometry.

D. Magnetic Properties

For α-$MoTe_2$ a diamagnetic susceptibility $\chi = -110 \times 10^{-6}$ emu/g-atom Mo was obtained, in agreement with data in the literature (*11*). For β-$MoTe_2$ a nearly temperature-independent paramagnetic susceptibility $\chi = +228 \times 10^{-6}$ emu/g-atom Mo was found.

Discussion

The experimental data of the previous section show that there exists a large difference between the properties of α- and β-$MoTe_2$. In this section these differences are discussed in terms of the energy levels for the electrons.

The properties of transition metal compounds depend to a large extent on the ligand-field splitting of the metal d orbitals. For a trigonal-prismatic coordination of the metal, two different models for the ligand-field splitting have been proposed in the literature. In one model (*12*, *13*) the state of lowest energy is a doubly degenerate e'*-level, in the other model (*5*, *14–16*) the lowest state is a nondegenerate $a_1'^*$ level. In order to clarify this point, crystal-field and molecular orbital calculations have been carried out (*17–19*).

The result of the calculations for a trigonal-prismatic coordination (symmetry D_{3h}) is shown in Fig. 4. The metal d-orbitals lead to the antibonding levels $a_1'^*$ (d_{z^2}), e'^* ($d_{x^2-y^2}$, d_{xy}) and e''^* (d_{xz}, d_{yz}) (z is the trigonal axis). The order of the levels depends on the angle θ between the z axis and the metal-ligand direction. In α-$MoTe_2$ $\theta = 48°15'$, in which case the $a_1'^*$ level is calculated to have the lowest energy.

Similar calculations were carried out for an octahedral coordination, with the metal atom shifted along the trigonal axis (symmetry C_{3v}) (*19*). This corresponds approximately to the coordination of the Mo-atoms in β-$MoTe_2$ (Fig. 1b). In this case one obtains two degenerate e^* levels, and a nondegenerate a^* (d_{z^2}) level, the lowest level being an e^* level.

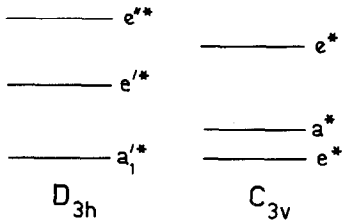

FIG. 4. Ligand field splitting of d orbitals for metal atoms with (a) a trigonal-prismatic coordination (symmetry D_{3h}), and (b) an octahedral coordination with the metal atom shifted along the trigonal axis (symmetry C_{3v}).

In $MoTe_2$ the metal atoms have a $(4d)^2$ configuration. The absence of local magnetic moments in $MoTe_2$ indicates that the low-spin state has the lowest energy. Thus, in α-$MoTe_2$ the two d electrons will occupy the $a_1'^*$-level.

In solids the d levels broaden into narrow energy bands, as a consequence of metal–ligand and direct metal–metal interactions. In addition to the narrow d bands, there are the valence and conduction bands, derived mainly from s and p orbitals of the ligand and the metal respectively. These bands are expected to be quite broad, because of the large overlap between s and p orbitals of the metal and the ligand atoms.

The semiconducting character of α-$MoTe_2$ and the metallic character of β-$MoTe_2$ follow quite naturally from these considerations (Fig. 5). In α-$MoTe_2$ the valence band and the $a_1'^*$ band are completely occupied by electrons, and all other bands are empty. The observed activation energy of the resistivity corresponds closely to half of the energy gap. Thus, in α-$MoTe_2$ the separation between the $a_1'^*$ and the e'^* bands must be at least

[2] The magnitude of the resistivity differs from sample to sample, depending on the quality of the sample, the conditions during pressing, etc. Figures 2 and 3 refer to different samples.

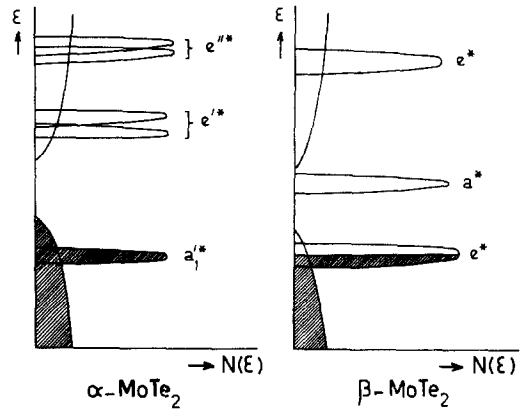

FIG. 5. Schematic energy level diagrams for α- and β-$MoTe_2$. Plotted is the energy ϵ of electronic states versus the density of states $N(\epsilon)$. Areas occupied by electrons are hatched. For α-$MoTe_2$ the splitting of the e'^* and e''^* bands due to spin-orbit coupling is indicated.

1.18 eV. In β-$MoTe_2$ the degenerate e^* band is only partly occupied, leading to metallic conductivity.

In the qualitative energy level diagram of Fig. 5 we assumed that the valence band overlaps the $a_1'^*$ band, and the conduction band overlaps the e'^* and e''^*-bands. This is based on the observation that the mobilities of electrons and holes in α-$MoTe_2$ (*5*, *11*), and also in the isostructural compounds MoS_2 (*5*, *20*) and WSe_2 (*21*) are quite large, and comparable to the mobilities of charge carriers in II–VI compounds such as ZnS (*22*), or in $SnSe_2$ (*23*). In our opinion, this indicates that the conduction in α-$MoTe_2$ is due to charge carriers in the broad valence and conduction bands, and not in the narrow *d* bands.[3]

Goodenough (*13*) has discussed the energy levels of WSe_2 and similar compounds with a trigonal-prismatic coordination of the metal atoms, assuming the e'^* states to have the lowest energy. The semiconducting character of WSe_2 is then explained by the spin-orbit splitting of the e'^* band in a filled band and an empty band. However, the spin-orbit coupling required to produce an energy gap of 1.35 eV [as is observed for WSe_2 (*21*)] between these two bands, is much larger than one expects from free-ion data for the spin-orbit coupling of 5*d* electrons of W^{4+}. For α-$MoTe_2$ the observed energy gap of 1.18 eV is certainly not due to a spin-orbit splitting of the e'^*-band. Therefore, in our opinion the semiconducting character of α-$MoTe_2$, MoS_2, $MoSe_2$ and WSe_2 can be understood only if the $a_1'^*$-state is the lowest metal *d* level.

The phase transition in $MoTe_2$ shows that the trigonal-prismatic coordination of the metal atoms (α-$MoTe_2$) has a lower energy than the octahedral coordination (β-$MoTe_2$). From electrostatic considerations one would expect the octahedral coordination to be more stable (*28*). Molecular-orbital calculations show that for atoms with configurations d^0, d^1, and d^2 the *d* covalency, i.e., the overlap of metal *d* orbitals with ligand orbitals, provides a stabilizing factor for the trigonal-prismatic coordination (*15*, *17*, *18*).

[3] Date on compounds, approximately isostructural with α-$MoTe_2$, also indicate an overlap of the $a_1'^*$ band with the valence band. Hall and Seebeck effect data of $TaSe_2$ and $NbSe_2$ indicate mixed conduction, i.e., by electron and holes (*24*, *25*). Similar conclusions were obtained for NbS_2, TaS_2, and $TaTe_2$ (*26*, *27*).

From the position of the plasma edge in NbS_2 and $NbSe_2$ an effective mass of $m^* \simeq 2m_0$ is calculated (*5*). For the states of the narrow $a_1'^*$ band (the width was estimated to be about 0.5 eV (*5*)) considerably larger values of m^* are expected. Therefore, the low values of m^* indicate conduction in a broad band, i.e., an overlap of the $a_1'^*$ band and the valence band.

From data on the thermoelectric power of *n*-type MoS_2, one can estimate the effective mass $m^* \simeq m_0$. This indicates that at least in this compound, *n*-type charge carriers occupy states of the broad conduction band.

Acknowledgment

This investigation was supported by the Netherlands Foundation for Chemical Research (SON) with financial aid from the Netherlands Organization for the Advancement of Pure Research (ZWO).

References

1. B. I. Halperin and T. M. Rice, *Solid State Phys.* **21**, (1968).
2. D. Adler, *Solid State Phys.* **21**, (1968).
3. Proc. int. conf. semiconductor-metal transitions, *Rev. Mod. Phys.* **40**, 673–839 (1968).
4. T. J. A. Popma and C. F. van Bruggen, *J. Inorg. Nucl. Chem.* **31**, 73 (1969).
5. J. A. Wilson and A. D. Yoffe, *Advan. Phys.* **18**, 193 (1969).
6. M. Spiesser and J. Rouxel, *C.R. Acad. Sci. (Paris)* **265**, 92 (1967).
7. D. Puotinen and R. E. Newnham, *Acta Crystallogr.* **14**, 691 (1961).
8. B. E. Brown, *Acta Crystallogr.* **20**, 268 (1966).
9. E. Revolinsky and D. J. Beerntsen, *J. Phys. Chem. Solids* **27**, 523 (1966).
10. S. Kabashima, *J. Phys. Soc. Japan* **21**, 945 (1966).
11. A. Lepetit, *J. Phys.* **26**, 175 (1965).
12. K. Koerts, Dissertation, Leiden, 1965.
13. J. B. Goodenough, *Mater. Res. Bull.* **3**, 409 (1968).
14. F. Hulliger, *Struct. Bonding Berlin* **4**, 83 (1968).
15. R. Huisman, R. de Jonge, and C. Haas, *Third Int. Conf. Solid Compounds Transition Elements, Oslo* (1969).
16. K. Anzenhofer, J. M. v.d. Berg, P. Cossee, and J. N. Helle, *J. Phys. Chem. Solids*, to be published.
17. R. Huisman, R. de Jonge, C. Haas, and F. Jellinek, to be published.
18. R. Huisman, Dissertation, Groningen, 1969.
19. R. de Jonge, Dissertation, Groningen, 1970.
20. R. Fivaz and E. Mooser, *Phys. Rev.* **163**, 743 (1967).
21. L. C. Upadhyayula, J. J. Loferski, A. Wold, W. Giriat, and R. Kershaw, *J. Appl. Phys.* **39**, 4736 (1968).
22. B. Ray, "II–VI Compounds," Pergamon Press, Oxford, 1969.
23. G. Busch, C. Frohlich, and F. Hulliger, *Helv. Phys. Acta* **34**, 359 (1961).
24. H. N. S. Lee, H. McKinzie, D. S. Tannhauser, and A. Wold, *J. Appl. Phys.* **40**, 602 (1969).
25. H. N. S. Lee, M. Garcia, H. McKinzie, and A. Wold, *J. Solid State Chem.* **1**, 190 (1970).
26. M. H. van Maaren and H. B. Harland, *Third Int. Conf. Solid Compounds Transition Elements, Oslo* (1969).
27. M. H. van Maaren and H. B. Harland, *Phys. Lett. A* **29**, 571 (1969).
28. R. J. de Munk, Afstudeerverslag, Technical University, Delft, 1967.